The International Journal of Advanced Manufacturing Technology
https://doi.org/10.1007/s00170-018-3108-1

ORIGINAL ARTICLE

Analysis of deposition sequence in tool-path optimization for low-cost material extrusion additive manufacturing

Neri Volpato [1] · Thiago Tavares Zanotto [1]

Received: 15 August 2018 / Accepted: 20 November 2018

Abstract
This study draws attention to the issue of how sensitive a low-cost 3D printer is to the material deposition sequence, when trying to speed up the process by applying tool-path optimization. The objective was to evaluate the influence of some changes in the deposition sequence on the mechanical properties, dimensional variation, and building time of specimens manufactured in polylactic acid (PLA). To achieve that, three deposition strategies were planned considering different deposition sequences, with and without optimization. An experiment involving an interruption of the extrusion nozzle was also designed to analyze the influence of idle time during material deposition. The material properties were evaluated by tensile and three-point bending tests. The results showed that a longer idle time between adjacent raster segments caused material cool-down, which, in this study, decreased the tensile strength by 35% and the flexural strength by 46%. Therefore, in a low-cost 3D printer, if the user does not pay attention to the deposition sequence during tool-path optimization, the mechanical property of the material can be badly affected. Additionally, the optimized intercalated deposition sequence allowed for savings of up to 42.7% in manufacturing time, and no expressive dimensional variation was found between the deposition strategies.

Keywords Tool-path optimization · Deposition sequence optimization · Process planning · Additive manufacturing · Material extrusion

1 Introduction

Additive manufacturing (AM) based on material extrusion uses an extrusion nozzle moving in the XY plane to deposit a filament of material in each layer of the part [1]. Fused Deposition Modeling (FDM), developed by Stratasys Ltd. was the first material extrusion AM technology available on the market. Manufacturing time is particularly important for this kind of technology because the extrusion nozzle must produce a filament to fill in entire areas of each layer following a tool-path [2].

The tool-path in material extrusion AM technology is composed of contours (C), which limit the areas to be filled with material, and an internal filling. The internal filling is usually performed using a zigzag strategy, also known as raster filling, containing segments with a start and endpoint [2, 3]. When a C is formed by a non-convex polygon, a single continuous raster segment (CRS) is not sufficient to fill in the entire area [4]. The same thing happens when there is an internal C in the geometry. Therefore, more than one CRS is required in these cases. Figure 1(a) schematically shows the results of path planning with a possible deposition sequence of Cs and CRSs. In this example, C3 and C1 require three and two CRSs, respectively, to be filled. These characteristics cause the tool-path to not be performed continuously, and the extrusion nozzle needs to jump from one point to another (C and CRS) to start a new deposition. This head repositioning (also known as non-productive airtime or jumps) is represented as dashed lines in Fig. 1. More details about this and other parts of a tool-path, which affect build time, can be found in [4–7].

The deposition sequence also must consider some precedence constraint aspects. For instance, the material addition in

✉ Neri Volpato
nvolpato@utfpr.edu.br

Thiago Tavares Zanotto
thiagozanotto@hotmail.com

[1] Department of Mechanical Engineering, Federal University of Technology - Paraná (UTFPR), R. Deputado Heitor Alencar Furtado, 5000-CEP, Curitiba, PR 81280-340, Brazil

Published online: 26 November 2018

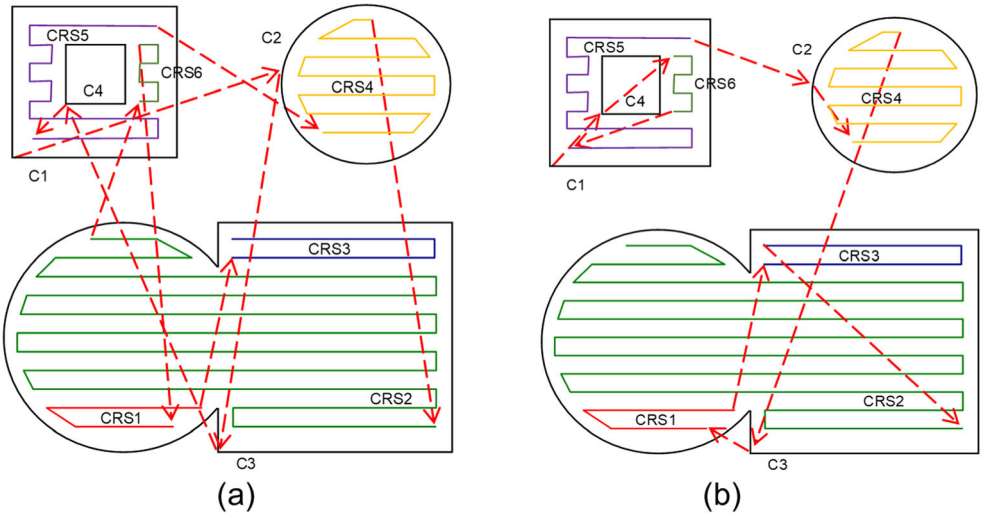

Fig. 1 Schematic of a path planning showing the discontinuity in sequential (**a**) and intercalated (**b**) material deposition strategies

FDM technology is usually performed by first depositing all contours of one layer, and only after this, the internal areas of each contour are added. This precedence option is referred to here as a sequential deposition, i.e., first all Cs are deposited and then all CRSs (Fig. 1a shows the sequence: C1, C2, C3, C4, CRS5, CRS4, CRS2, CRS6, CRS1, and CRS3). Another option would be an intercalated deposition, where right after an external C of the part is added, its specific CRSs can be deposited. Figure 1(b) shows one possible intercalated sequence: C1, C4, CRS6, CRS5, C2, CRS4, C3, CRS1, CRS3, and CRS2. In this option, any existing internal C must be deposited before its respective CRSs (see C1 and C4 in Fig. 1b). This precedence aspect is relevant because it can reduce the repositioning distance substantially, therefore reducing the time in path planning.

There are some studies on tool-path optimization in the material extrusion AM specifically in the deposition sequence. Wah et al. [8] combined genetic algorithms incorporating 2-opt and 3-opt local optimization and integer programming to address the problem. Weidong [9] also presented an optimization solution using genetic algorithms but focused on solving the optimization of C paths. Dreifus et al. [10] proposed a graph theoretical approach to design a tool-path algorithm that, according to them, gives a minimal time path for an arbitrary single-bead-wide print. Volpato et al. [3] considered C and CRSs in the proposed algorithms to reduce head repositioning, with the results showing great potential to speed up the process. In a slightly different and clever approach, Lensgraf and Mettu [11] proposed reducing the idle time by defining a tool-path that maintains the printer on a local island for some layers and then jumps to the next island using a greedy method. The authors reported a substantial savings in head repositioning.

Although the above studies proposed different approaches, none of them presented discussions regarding the influence of such tool-path optimization on the part properties. This influence is relevant because changes in

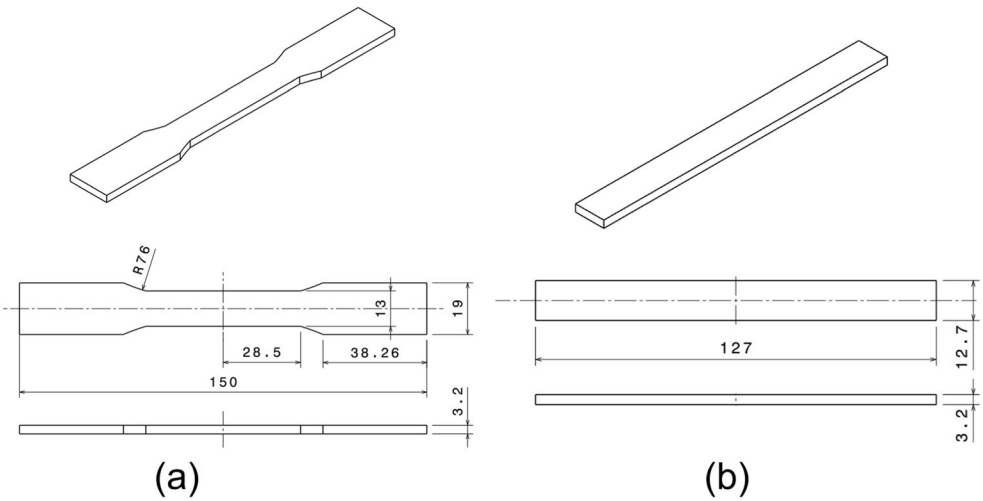

Fig. 2 Dimensions (mm) of the (a) tensile and (b) bending specimens

the deposition sequence can have some effects on the process. For instance, usually, a positive aspect when optimizing a tool-path is that the time between layers tends to be reduced. This is directly related to the material cooling, and, according to Faes et al. [12], as the time between layers is reduced, the material properties increase since the bonding between layers occurs at higher temperatures. Agarwala et al. [4] highlighted that weak interfaces between adjacent filaments (roads) and layers can occur due to the build strategy, i.e., raster fill pattern. The authors emphasized that since the deposition of non-continuous raster segments is not always sequential and adjacent, there is the possibility of excessive substrate cooling in regions between two adjacent raster lines of two different raster segments. The substrate cooling may result in insufficient bonding between the adjacent roads, thus weakening the filament interfaces. Other researchers also highlighted these findings. Sun et al. [13] reported that the mechanical properties of the parts were negatively influenced by the insufficient bond strength between filaments and that this bond formation is driven by the thermal energy of the extruded material. Huang [14] also claimed that complete de-bonding between adjacent roads is also associated with high substrate cooling. Gurrala and Regalla [15] concluded that the manufacturing strategy and environment temperature are key factors that affect both the quality and the bond strength between filaments.

In general, the main suggestion found to reduce these thermal effects is to keep the environment temperature inside the building chamber above a threshold for each specific material, not allowing it to drop below that value [4, 13–15]. This is the solution adopted by FDM; however, it is not the case for most low-cost desktop technologies which, at most, have a heated bed and a closed chamber.

As it can be observed, it is possible to speed up the material extrusion AM technology by applying optimization algorithms to define the best deposition sequence for the tool-path segments, but its influence on the final part must be analyzed. The objective of this research is to study this influence on mechanical properties, dimensional variation, and build time for specimens manufactured using a low-cost desktop 3D printer, which is based on the material extrusion principle.

Table 1 Process parameters used for all proposed strategies

Parameters	Values
Nozzle diameter	0.4 mm
Feedstock diameter	1.75 mm
Gap	0 (fill density 100%)
Layer thickness	0.25 mm
Head speed	40 mm/min
Printing temperature	200 °C
Raster angle	0°/90°

2 Materials and methods

To achieve the objectives of this study, five test specimens for each proposed deposition strategy (described below) were built in polylactic acid (PLA) and subjected to tensile and three-point bending tests. The printer used was a 3D Cloner, which does not have chamber temperature control or a heated bed (platform). This equipment is one of various low-cost AM machine available on the market. The tensile and bending dimensions of the specimens (Fig. 2) follow the ASTM D638-14 [16] and ASTM D790-10 [17], respectively. Tensile and three-point bending tests were performed in an EMIC DL-1000 test machine. The main printing parameters used can be seen in Table 1, and they were constant for all proposed strategies. The process planning software used was Simplify3D.

The building time was registered directly from the 3D printer. The dimensional measurements were performed using a Mitutoyo 150-mm digital caliper with 0.01-mm resolution.

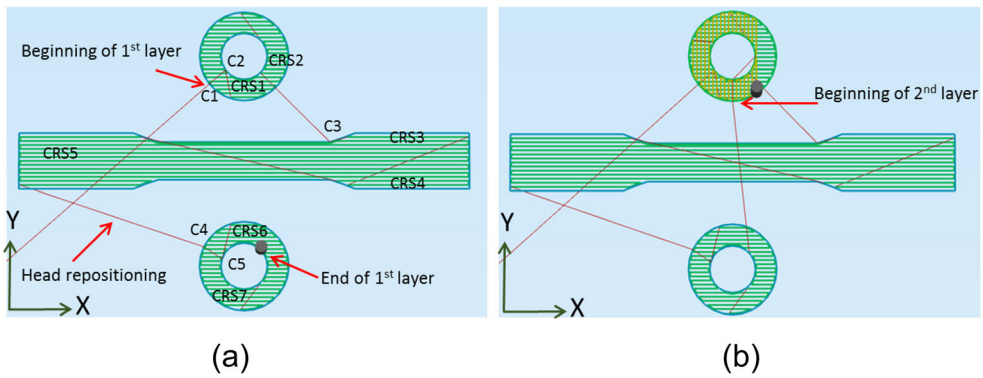

Fig. 3 Schematic of the tool-path deposition for the CRCR-NO. (**a**) First layer. (**b**) Start of the second layer

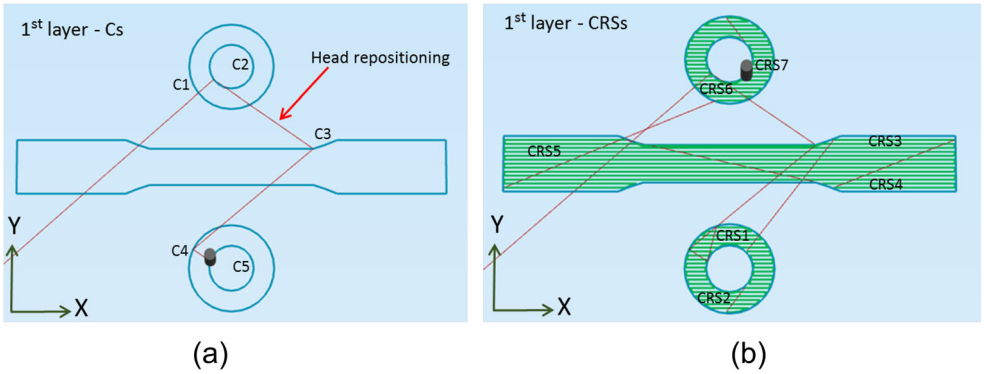

Fig. 4 Tool-path deposition for the CCRR-O first layer. (**a**) All Cs first. Then (**b**) all CRSs

2.1 Proposed deposition strategies to study tool-path optimization

For this study, three different deposition strategies were defined, identified as non-optimized and optimized intercalated deposition, and optimized sequential deposition. The first two strategies were chosen based on their common use in low-cost 3D printers. The third was chosen due to it being commonly used in Stratasys machine.

The optimization heuristic used was the basic greedy method. This heuristic starts from the origin point, and then, it adds the point belonging to a C (or CRS) to the route in every step that has not yet been visited, and in which the distance to the last point visited is the shortest possible. Both points (start and end) of a CRS are analyzed in this process, and when the closest is found, the other is automatically included as being the end point of this specific CRS [3].

The tensile and bending specimens were manufactured concurrently using two shims (Fig. 3) of 30-mm external and 15-mm internal diameter, and 3.2-mm thickness. These shims were added to the build to increase the number of Cs and CRSs in each layer, thus increasing the possibility of the tool-path optimization influencing the results.

2.1.1 Non-optimized and optimized intercalated deposition (CRCR-NO and CRCR-O)

The deposition sequence in this strategy was already described in Sect. 1. A notation CRCR was applied to help identify this strategy, where a *C* is followed by one or more CRSs (for simplicity, it will be represented only by the letter *R*), and then, the next *C* is followed by another *R* and so on. The complement NO in this notation means not applying tool-path optimization (CRCR-NO). When non-optimization of the head repositioning was used, the tool-paths (sequence of Cs and CRSs) for the first and second layer were the same for the third and fourth layer, and so on. Figure 3 shows the tool-path of the first layer and the start of the second layer for this strategy. The raster angles for the first and second layers were 0 (zero) and 90°, in relation to the *x*-axis, respectively.

In the optimized intercalated sequence strategy (CRCR-O), the last CRS of a layer is the starting point of the next layer, thus reducing the chance of tool-path repetition throughout the part.

2.1.2 Optimized sequential deposition (CCRR-O)

As previously mentioned, this strategy involves depositing all Cs of a layer first and only then the CRSs are deposited. This

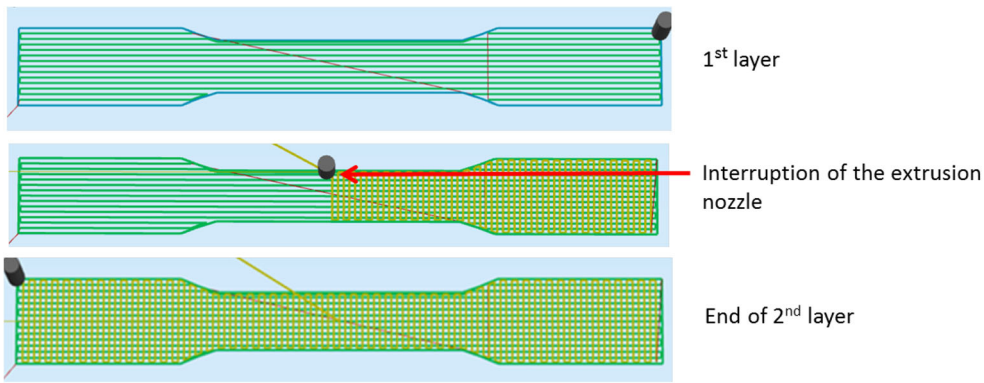

Fig. 5 Illustration of the tool-path with the intentional interruption of the extrusion nozzle

Table 2 Comparison of build time for the proposed strategies

Specimens	CRCR-NO (s)	CRCR-O (s)	Variation (%)	CCRR-O (s)	Variation (%)
Tensile	3139	3135	− 0.13	4452	+ 41.8
Bending	2392	2383	− 0.38	3377	+ 41.2

strategy used tool-path optimization. Figure 4 shows the path planning of the first layer using this strategy.

2.2 Tool-path planning considering an intentional extrusion break

An additional experiment was performed introducing an intentional interruption (delay) of the material extrusion during the CRS in the transverse layers, in both tensile and bending specimens. In Fig. 5, an illustration of this experiment is presented. As it can be seen, the deposition in the odd layers (raster angle 0°) is done normally, but in the even layers (raster angle 90°), there is an interruption of the material extrusion in the middle of the part. After the interruption, the extrusion nozzle goes to the platform corner and waits there until the deposition restarts. This was done to avoid irradiation of the nozzle over the specimen during this idle time. Two delays were defined, 65 (P65) and 17 s (P17). The 65-s delay was chosen because it corresponds to the estimated time to deposit 50% of the CRS in the transverse layer. The 17-s delay was an estimated time for the extrusion nozzle to go to the origin position and return, which, in this case, was the upper left corner of the platform.

The main goal of this experiment was to evaluate the influence of idle time (material cooling) on the bonding between adjacent filaments of adjacent CRSs. This is relevant since tool-path optimization will change the time between the filling of these adjacent CRSs. The shims were not manufactured concomitantly in these experiments, and the non-optimized intercalated deposition sequence was used. The notations used for these analyses were CRCR-NOP17 and CRCR-NOP65.

After the tensile and three-point bending tests, the fracture morphology of the CRCR-NOP17 and CRCR-NOP65 specimens was analyzed using a TM 3000 (Hitachi) scanning electron microscopy (SEM).

3 Results and discussion

Table 2 presents the build time to manufacture the tensile and bending specimens (with the shims) for the proposed strategies. The variations (%) shown in this table are related to the CRCR-NO strategy.

It can be observed that, for this specific build, no time was saved by the optimization, i.e., no variation between the CRCR-NO and CRCR-O strategies. On the other hand, the build time increased around 41% for the sequential deposition CCRR-O when compared to the intercalated (CRCR-NO). This is directly related to the logic applied by this strategy (CCRR-O), which normally generates more idle movements or repositioning, since it must go through all Cs, before starting the CRSs.

Table 3 shows the dimensional results for all strategies tested, including the strategy with interruption of the extrusion.

The results for the tensile specimens showed that the maximum width variation was approximately 3.7% for the CRCR-O strategy, regarding the nominal dimensions (Fig. 2). Regarding thickness, the highest variation was approximately 5% for the P65 strategy. Considering the mean and standard deviation, the dimensional differences between CRCR-NO, CRCR-O, and CCRR-O strategies were not significant.

For the bending specimens, the CRCR-O strategy presented the highest width variation (3.3%), when comparing nominal values. CRCR-NOP17 and CRCR-NOP65 strategies presented the highest thickness variation (2.8% and 2.5%, respectively). Regarding the length, the variation found was not significant, not exceeding 0.5% in relation to the nominal dimension.

Figure 6 shows the results for the tensile test. The highest value (mean) of the ultimate tensile stress was 50.4 MPa when the specimens were manufactured by the CCRR-O strategy. The mean decreased by 5% for the CRCR-O. However, considering the mean and standard deviation of the results for the

Table 3 Dimensional results for all proposed strategies (five specimens per strategy)

	Tensile specimen		Bending specimen		
Strategy	Width (mm)	Thickness (mm)	Width (mm)	Thickness (mm)	Length (mm)
CRCR-NO	13.26 ± 0.09	3.21 ± 0.05	12.87 ± 0.07	3.19 ± 0.04	126.87 ± 0.10
CRCR-O	13.47 ± 0.04	3.19 ± 0.02	13.12 ± 0.24	3.17 ± 0.08	127.15 ± 0.05
CCRR-O	13.26 ± 0.09	3.25 ± 0.04	12.74 ± 0.07	3.20 ± 0.05	126.47 ± 0.39
CRCR-NOP17	13.21 ± 0.04	3.31 ± 0.02	12.68 ± 0.03	3.29 ± 0.02	126.69 ± 0.04
CRCR-NOP65	13.15 ± 0.06	3.36 ± 0.04	12.71 ± 0.07	3.28 ± 0.06	126.73 ± 0.16

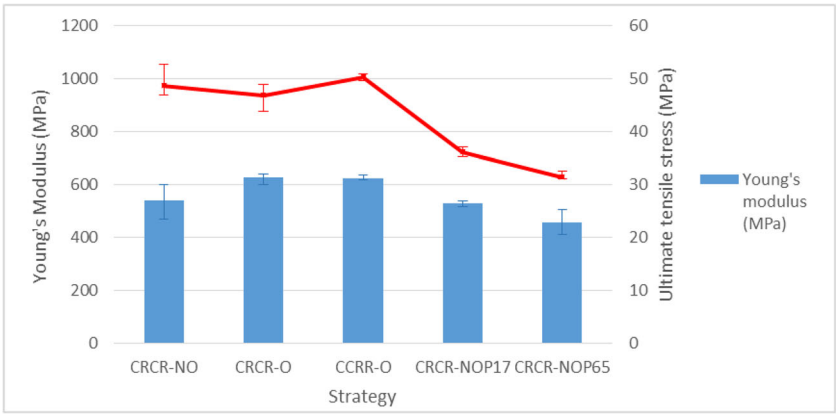

Fig. 6 Young's modulus and ultimate tensile stress from the tensile tests

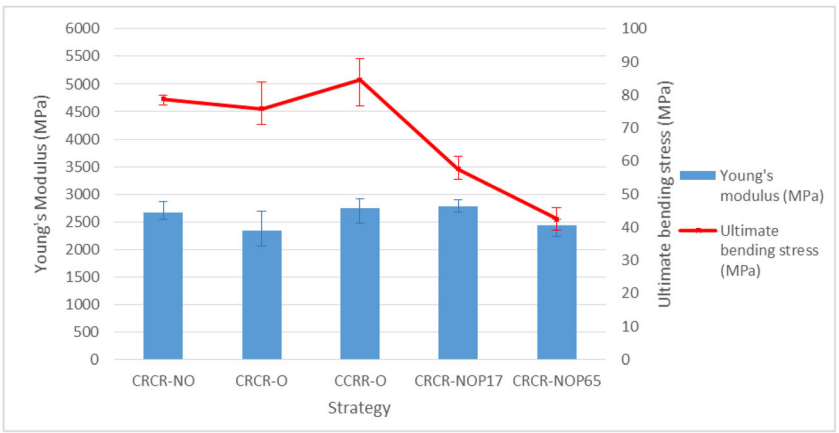

Fig. 7 Young's modulus and ultimate bending stress from the three-point bending test

CRCR-NO, CRCR-O, and CCRR-O strategies, the values are comparable and presented little variation among them.

On the other hand, a decrease of approximately 25% and 35% was observed when comparing CRCR-NOP17 and CRCR-NOP65 (both with extrusion interruption) with the CRCR-NO strategy. The modulus of elasticity also decreased for these two strategies. As the only change in the process was the interruption during deposition (delay between the CRSs), it can be concluded that the bonding between the adjacent filaments was not efficient and that this was the reason for this decrease in the material property. This corroborates the main idea found in the

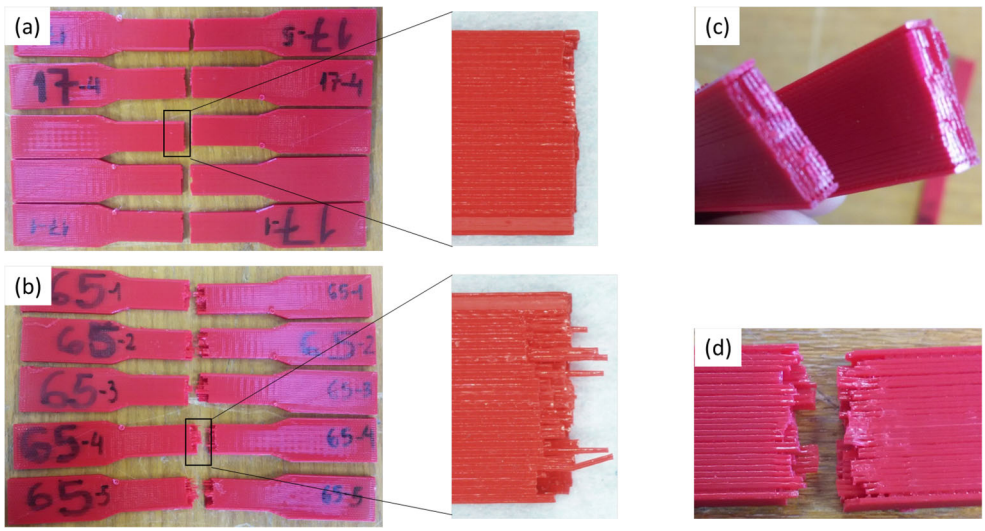

Fig. 8 Specimens (**a**) CRCR-NOP17 and (**b**) CRCR-NOP65 after tensile tests, and (**c**) CRCR-NOP17 and (**d**) CRCR-NOP65 after bending tests

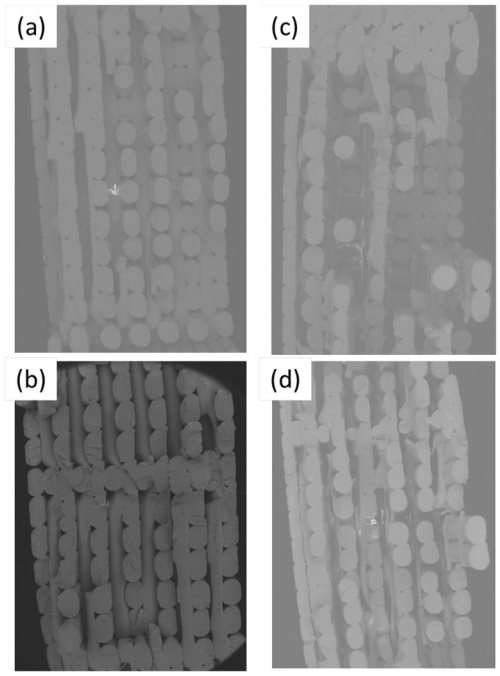

Fig. 9 SEM images of the fractured surfaces of tensile specimens. (**a**) CRCR-NOP17 and (**b**) CRCR-NOP65, and bending specimens (**c**) CRCR-NOP17, and (**d**) CRCR-NOP65

literature, in which the contact temperature is critical for a good neck formation between adjacent filaments [4, 13–15].

Figure 7 shows the results of the three-point bending tests for the proposed strategies. The highest mean value for the ultimate bending stress was 84.64 MPa using the CCRR-O strategy, with a decrease of approximately 7% and 10% for the CRCR-NO and CRCR-O strategies, respectively. However, considering the mean and standard deviation values, the results obtained were similar.

In general, the sequential deposition CCRR-O yielded parts slightly stronger than the intercalated deposition. So far, a reasonable explanation for this behavior has not been found.

Comparing CRCR-NOP17 and CRCR-NOP65 to CRCR-NO again, the decrease in flexural strength was approximately 26% and 46%, respectively. The 20% decrease shows that increasing the delay from 17 to 65 s has a direct correlation with the decrease in strength. The difference in the modulus of elasticity was not so evident. The interruption during filament deposition affected the bonding between adjacent filaments, which caused significant influence on the mechanical behavior of the material, as observed in the tensile tests.

Figure 8 shows some specimens after the tensile and three-point bending tests for the CRCR-NOP17 and CRCR-NOP65 strategies. For both strategies, all fractures occurred exactly in the middle of the specimen, where the interruption occurred (this was not the case for the specimens without interruption). There is an evident difference in the fracture between these two strategies. For the CRCR-NOP65 specimen, some longitudinal filaments were exposed after rupture. These filaments were from the layers above and below the interrupted layer. This behavior suggests that, due to the long interruption time in the transverse layers, the material cooling also caused inefficient bonding of the filaments between adjacent layers.

The SEM images of the CRCR-NOP17 and CRCR-NOP65 fractured specimens, shown in Fig. 9, add to this analysis. First, as expected, the fracture morphologies showed that the filaments of the first layer (left side of the pictures), which are in contact with the machine platform, have a flatter cross-section when compared to those of the top layers, which are closer to an elliptical shape. The exposed longitudinal filaments mentioned become evident in the CRCR-NOP65 strategy (Fig. 9b, d), appearing isolated from the other filaments. In this same strategy, some filaments of a rather circular cross-section can be found, which means that they withstand the tensile stress isolated from each other. This indicates a filament that did not have a good interaction with its neighbors (both from the same layer and between layers). Some filament sets remained attached to each other, suggesting that they slid between the adjacent layers in this region (Fig. 9b and d).

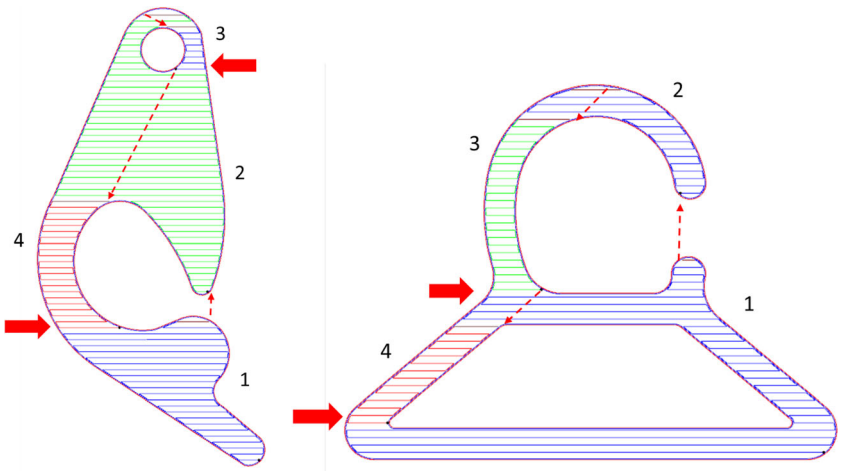

Fig. 10 Examples of parts where the deposition sequence may negatively affect the part strength in some critical points

Again, this is a sign of bad bonding between layers. These effects were not observed well in the CRCR-NOP17 strategy (Fig. 9a and c), which indicates that the temperature at the deposition after the interruption was higher.

Considering the manufacturing conditions of this study, the general results show that there was little variation between the strategies, with and without optimization of the head repositioning. However, for the tests with interruption, a considerable variation in the strength was observed. Based on that, it is possible to assume that, if a particular tool-path increases the deposition time between adjacent filaments in critical regions, the mechanical properties of the part will be negatively affected. Finding examples of part geometry where a naïve tool-path negatively affects their mechanical properties is not difficult. Figure 10 shows two examples in which the deposition sequence adopted compromises the material strength at the critical regions indicated by solid arrows. Therefore, it is strongly suggested that any tool-path optimization algorithm should consider the deposition time between adjacent filaments as a deposition constraint.

Finally, although up to now, this study has been done just with PLA, it is expected that similar effects would be observed with acrylonitrile-butadiene-styrene (ABS) or polyethylene terephthalate glycol (PETG), which are also popular in low-cost 3D printers. Furthermore, printers with additional features, such as a temperature controlled chamber or heated bed, will have smaller thermal gradients, especially for the first layers with the latter, but their efficiency needs to be studied. Further studies are under way to deepen the analysis of these aspects.

4 Conclusions

This study explored the influence of different deposition sequences, with and without head repositioning optimization, on the mechanical properties, dimensional variation, and build time of specimens produced with a low-cost material extrusion AM process.

Tool-path optimization did not yield any significant time savings in this study, probably because of the low number of contours and continuous raster segments in the build. On the other hand, the build time increased around 41% for the sequential deposition (CCRR-O), when compared to the intercalated strategy (CRCR-NO). This is directly related to the greater number of idle movements (repositioning) associated with the latter.

For the dimensional results, little variation was observed when comparing the tool-path with and without optimizations. Considering the mean and standard deviation, there was also little difference in the tensile and bending results between the strategies. However, for the experiments with the intentional interruption of the extrusion (17 and 65 s) in the middle of the specimen, a great decrease in the mechanical properties (25% and 35% for the ultimate tensile stress and 26% and 46% for the flexural strength, respectively) was found. This behavior was caused by the variation of material cooling (temperature) during filament deposition, considerably affecting the bonding between adjacent filaments. In the SEM analysis, it was also possible to observe that the adjacent layers did not undergo adequate bonding, contributing to the decrease in the tensile and bending strength results. The proposed method designed to analyze the influence of idle time on the mechanical properties was effective, enabling us to capture this effect. Further studies with different polymers and machine configurations (temperature controlled chamber, heated bed) are under way and will add valuable information to this subject.

Funding information This work was supported by the Coordenação de Aperfeiçoamento de Pessoal de Nível Superior (CAPES, Brazil) and Fundação Araucária do Paraná (Brazil).

Compliance with ethical standards

Conflict of interest The authors declare that they have no conflict of interest.

References

1. ISO/ASTM 52900 (2015) Additive manufacturing—general principlesTerminology
2. Gibson I, Rosen DW, Stucker B (2010) Additive manufacturing technologies. Springer, New York
3. Volpato N, Galvão LC, Nunes LF, Scanavini LG (2015) Combining heuristics for tool-path optimization in additive manufacturing, computer-aided production engineering - 23rd CAPE conference. University of Edinburgh, Edinburgh
4. Agarwala MK, Jamalabad VR, Langrana NA, Safari A, Whalen PJ, Danforth SC (1996) Structural quality of parts processed by fused deposition. Rapid Prototyping J 2:4–19
5. Han W, Jafari MA, Seyed K (2003) Process speeding up via deposition planning in fused deposition-based layered manufacturing processes. Rapid Prototyping J 9(4):212–218
6. Castelino K, D'Souza R, Wright PK (1999) Toolpath optimization for minimizing airtime during machining. J Manuf Syst 22(3):173–180
7. Jin Y-a, He Y, Xue G-h, Fu J-z (2015) A parallel-based path generation method for fused deposition modeling. Int J Adv Manuf Technol 77:927–937
8. Wah PK, Murty KG, Joneja A, Chiu LC (2002) Tool path optimization in layered manufacturing. IEEE Transactions 34:335–347
9. Weidong Y (2009) Optimal path planning in rapid prototyping based on genetic algorithm, Chinese Control and Decision Conference (CCDC 2009), pp. 5068–5072
10. Dreifus G, Goodrick K, Giles S, Patel M, Foster RM, Williams C, Lindahl J, Post B, Roschli A, Love L, Kunc V (2017) Path optimization along lattices in additive manufacturing using the Chinese postman problem. *3D*. Print Addit Manuf 4(2):98–104

11. Lensgraf S, Mettu RR (2016) Beyond layers: a 3d-aware toolpath algorithm for fused filament fabrication, IEEE International Conference on Robotics and Automation, May 2, pp. 3625–3631
12. Faes M, Ferraris E, Moens D (2016) Influence of inter-layer cooling time on the quase-static properties of ABS components produced via fused deposition modeling", 18th CIRP conference on electro physical and chemical machining, April, Tokyo
13. Sun Q, Rizvi GM, Gu P, Bellehumeur CT (2008) Effect of processing conditions on the bounding quality of FMD polymer filaments. Rapid Prototyping J 14:72–80
14. Huang B (2014) Alternate slicing and deposition strategies for Fused Deposition Modelling, Ph.D. Thesis, Auckland University of Technology, School of Engineering, January, 336p
15. Gurrala PK, Regalla SP (2014) Part strength evolution with bonding between filaments in fused deposition modelling. Virtual and Physical Prototyping 9:141–149
16. ATSM D638-14 (2014) Standard test methods for tensile properties of plastics, American society for testing and materials (ASTM) international
17. ATSM D790-10 (2010) Standard test methods for flexural properties unreinforced and reinforced plastics and electrical insulating materials, American society for testing and materials (ASTM) International